

Supplementary Information

Multifaceted Folding-Unfolding Landscape of TrpZip2 β -Hairpin and the Role of External Sub-pico-newton Mechanical Tensions

Nayana Edavan Chathoth, Aparna G Nair, and Padmesh Anjukandi*

*Department of Chemistry,
Indian Institute of Technology Palakkad,
Kozhippara P. O., Kerala, India.*

Contents

I. System Details	3
II. Interaction Between TrpZip2 β-Hairpin and Water	4
III. Simulation Details	6
A. Molecular Dynamics Simulations	6
B. Steered Molecular Dynamics Simulation	6
C. TrpZip2 β -Hairpin Under the Influence of Uniform External Forces	7
D. Metadynamics Simulation	8
IV. Convergence of Metadynamics Simulation	11
A. TrpZip2 β -Hairpin in Solvent	11
B. Hairpin in Solvent and Under the Influence of a 30 pN External Tensile Force	13
C. Under the Influence of Uniform Force of Random Orientation	15
V. Comparison of the Free Energy Landscape Under Varying External Force Scenarios	17
VI. TrpZip2 β-Hairpin and its Folding-Unfolding Mechanism	19
A. TrpZip2 β -Hairpin in Solvent	19
B. Hairpin in Solvent and Under the Influence of a 30 pN External Tensile Force	22
C. Hairpin in Solvent and Under Uniform Forces of Random Orientation	25
References	28

I. SYSTEM DETAILS

TrpZip2 is an extensively studied β -hairpin structure synthesized by Crochan et.al.¹ This hairpin, with a sequence SWTWENGKWTWK NH₂, exhibits exceptional stability in the absence of metal bonds or disulfide linkages. The hairpin structure consists of six backbone hydrogen bonds and a hydrophobic core comprising two pairs of Tryptophan residues (TRP2-TRP11 and TRP4-TRP9) accounting for their high stability. Their folding mechanism has been well investigated and it is widely observed that they fold heterogeneously with various proposed mechanisms like zip-in, zip-out and middle-out mechanisms^{2,3}.

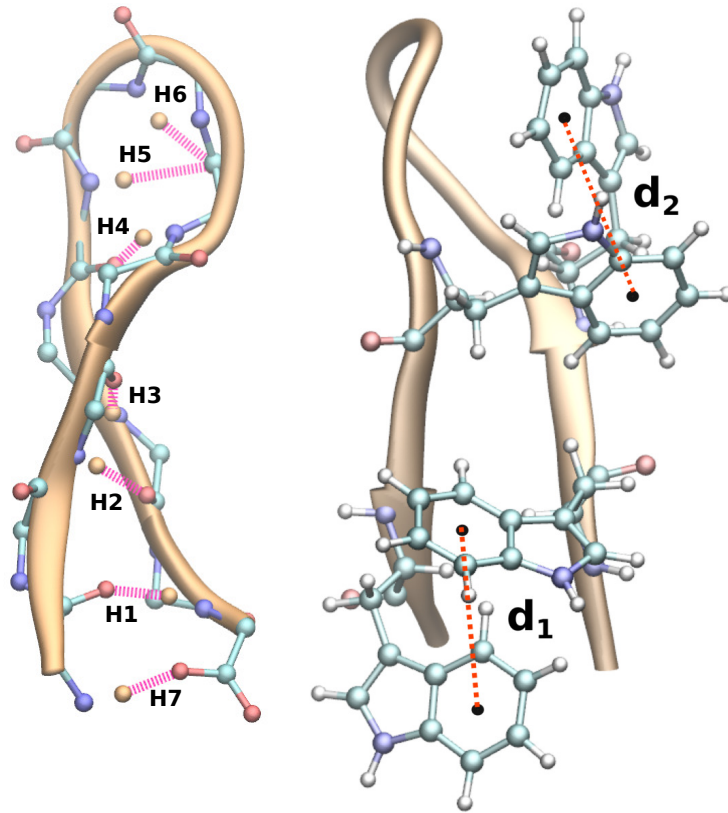


FIG. S1: Schematic representation of TrpZip2 hairpin protein (SWTWENGKWTWK NH₂), a 12 residue polypeptide β -Hairpin. The possible six backbone H-bonds (H_n, n ranging from 1-6), salt bridge interactions (H₇) and the two possible hydrophobic interactions (d_n, n ranging from 1-2) which holds the β -Hairpin intact are shown. We will be referring to the order of the bonds and hydrophobic interactions described herein for further discussion.

II. INTERACTION BETWEEN TrpZip2 β -HAIRPIN AND WATER

Protein folds and unfolds instinctively to form unique three-dimensional structures. A comprehensive understanding of protein folding can only be obtained by considering the forces acting on it by the environment in which they exist as the mechanism and also the rate at which a protein fold could hugely depend on the magnitude of the external forces. Numerous studies point to the origin of these forces to be attributed to the solvent molecules and that these solvent molecules exert a force (solvent-induced force) on the hydrophilic groups of the proteins.⁴⁻⁶ Thus one cannot neglect the solvent surrounding the protein and the forces exerted by these solvent molecules on them. Hence studying the protein folding without taking into account the forces experienced by the solvent molecules may be insufficient in rendering the exact mechanisms. The solvation pattern around each residue of TrpZip2 were calculated using the radial distribution function and depicted in Fig.2 in the main manuscript. The varying solvation environment could be a reason for the uneven distribution of forces around them which could be manifested in their folding-unfolding pattern. We thus quantify the non-bonded interaction between the solvent molecules and each residue of the protein and the results are shown in Fig. S2.

The non-bonded interaction energy is the sum of van der Waals and coulombic interaction energy and is given by the following equation

$$V_{total}(r_{ij}) = \left(\frac{C_{ij}^{(12)}}{r_{ij}^{12}} - \frac{C_{ij}^{(6)}}{r_{ij}^6} \right) + \left(\frac{q_i q_j}{4\pi\epsilon_0 r_{ij}} \right) \quad (1)$$

The differential of equation (1) with respect to r gives the force given by equation (2).

$$F_{total}(\mathbf{r}_{ij}) = \left(12 \frac{C_{ij}^{(12)}}{r_{ij}^{13}} - 6 \frac{C_{ij}^{(6)}}{r_{ij}^7} \right) \frac{\mathbf{r}_{ij}}{r_{ij}} + \left(\frac{q_i q_j}{4\pi\epsilon_0 r_{ij}^2} \right) \frac{\mathbf{r}_{ij}}{r_{ij}} \quad (2)$$

One can see from Fig. S2 that the coulomb and LJ potential and hence the force experienced by each residue is different. The hydrophilic groups near the ends and turns experience a greater force than the hydrophobic groups. We thus quantify the non-bonded interaction energies between the solvent and each residue of TrpZip2 β -Hairpin and identify that any change in the solvent structure and hence the interaction energy near the residue could very well alter the external force acting on them.

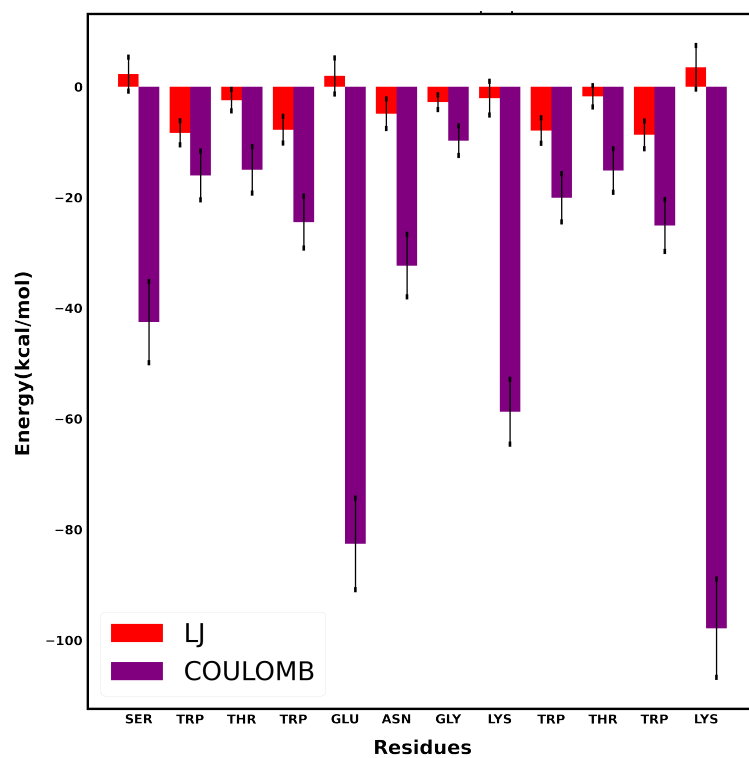


FIG. S2: The total non-bonded interaction energies between each residue of TrpZip2 β -Hairpin and water molecules.

III. SIMULATION DETAILS

A. Molecular Dynamics Simulations

The protein hairpin structure was obtained from Protein Data Bank (PDB ID:1LE1.pdb)⁷. The hairpin was placed in a box of 8.0 x 8.0 x 8.0 nm³ and solvated with 17043 SPC/E⁸ water molecules. In addition to the solvent, 2 Na⁺ and 3 Cl⁻ ions were also added to the peptide system in order to keep the system neutral. After the initial minimization (1000 steps using the steepest descent algorithm), 2 ns equilibration was performed. All simulations were carried out with GROMACS-4.5.5^{9,10} software suite. The OPLS-AA all-atom force field^{11,12} was applied for simulating the molecules. This combination of the forcefield and water model was chosen over their success in demonstrating the folded states in the previous works.^{13,14} Simulations were run in the NVT ensemble with periodic boundary conditions. The temperature of the system was kept constant at 300 K by coupling to a Nosé–Hoover thermostat.^{15,16} An integration time step of 2 fs was used and trajectory coordinates were recorded every 200 fs for analysis. All bond lengths were constrained using LINCS.¹⁷ The long-range electrostatics were accounted using the particle mesh ewald method¹⁸ with a coulomb cut-off of 1 nm and a 1 nm cut-off was used for van der Waals interaction.

B. Steered Molecular Dynamics Simulation

A series of constant-force Steered Molecular Dynamics (SMD)^{19,20} simulations were performed on TrpZip2 β -Hairpin to determine the response of end-to-end displacement of the hairpin with respect to the end tensile force. To apply the pull code integrated with GROMACS-4.5.5, one-dimensional tensile force were applied at the C_α atoms of the end residues (pull groups) of the hairpin along the +x and -x directions of the simulation box. To study the force-extension behavior of the hairpin, tensile forces ranging from 0 pN to 75 pN with a 15 pN interval were applied along the pull-groups. Once the pulling potentials were applied, the system was equilibrated for 2 ns before starting the SMD simulations. SMD simulation for a time period of 10 ns were performed in each case. The end to end distance (Q) was measured and we identify 30 pN end force as the maximum force to confine the hairpin to its folded state for a considerable interval of time without disturbing its morphology and beyond which the hairpin unfolds instantaneously. The evolution of the end to end

distance of the hairpin with respect to the varying external tensile forces is shown in Fig. S3.

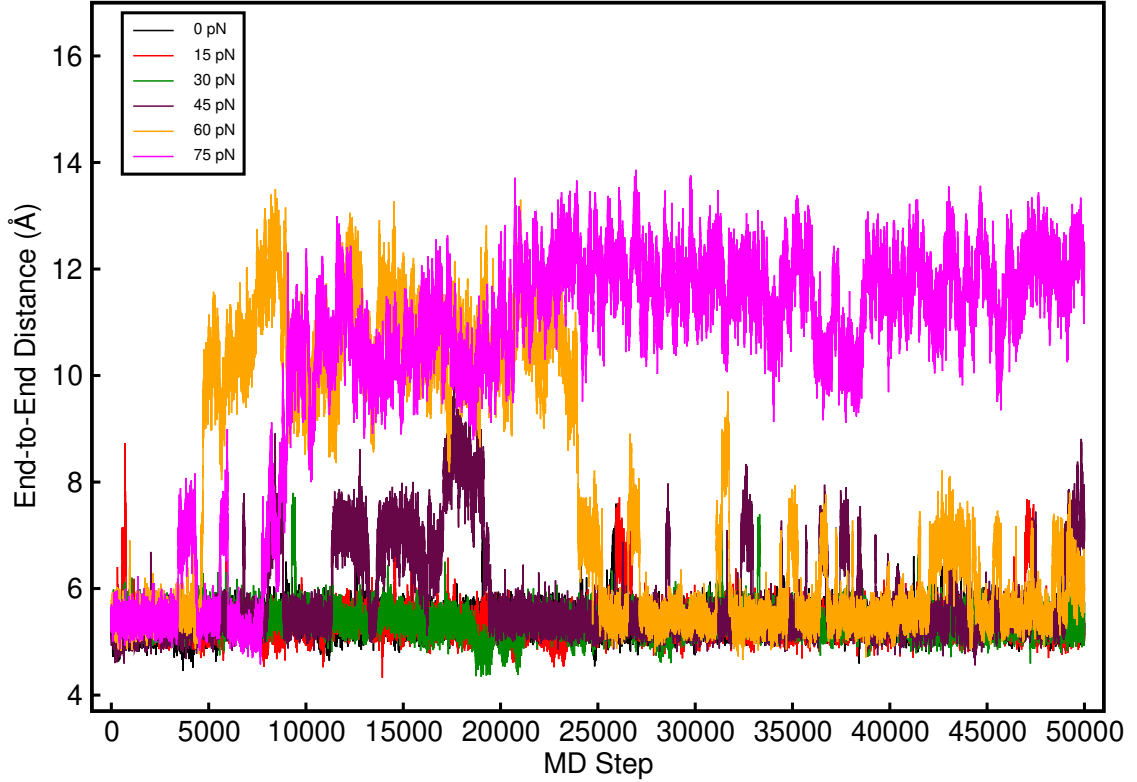


FIG. S3: Time evolution of the end to end distance of TrpZip2 β -Hairpin protein (SWTWENGKWTWK NH₂) as a function of different tensile stress ranging from 0-75 pN, at a temperature of 300 K and over a trajectory of 10 ns. The colour code for different end forces are provided in the legend.

C. TrpZip2 β -Hairpin Under the Influence of Uniform External Forces

In view of the fact that molecules in the solution phase appear to be subjected to random forces of ~ 4 - 5 pN induced by thermal fluctuation of nearby water molecules, we applied a force of 4 pN to each residue of the TrpZip2 β -Hairpin. The forces were applied in random orientations on the C_α atoms of all the residues except at the turn, so that the net external bias experienced by the hairpin was almost zero. This scenario of the protein being under the influence of random small forces by water yet again mimics the zero external bias on the protein.

D. Metadynamics Simulation

A widely popular computational technique employed in different fields such as biophysics, chemistry, and material science, molecular dynamics (MD) provides insights into a variety of domains ranging from protein folding to biomedicine. Due to the fact that most of the reactions of interest are sentient processes characterized by slow motions and that the MD time step often falls in the femtosecond range, MD tends to produce valid results only when it is run over a longer time scale to sample all the pertinent states. This limitation of MD can be conquered if one approach methods where the rare events can be accelerated within a shorter time scale with enhanced efficiency. To accelerate the sampling speed, often advanced sampling techniques are employed which includes Metadynamics (MTD), Replica exchange Molecular Dynamics (REMD), etc. In the current study we utilized Well-tempered Metadynamics (MTD)²¹ simulations which is an advanced sampling technique that is efficient in various fields like crystallography²², protein folding²³ to name a few. MTD involves the filling up of the potential energy landscape by adding a bias potential ($V_B(S,t)$) in the form of Gaussian functions of finite width along certain collective variables (CVs). The bias potential is added in a history-dependent manner such that visiting previous states of the system is prohibited thus facilitating the crossing of the energy barrier in the FES and effectively forming a flat surface which enables the system to take up all the physically relevant conformations.

(i) Choosing CVs

An important aspect of MTD simulation is the selection of the appropriate CVs. We call CVs (or degrees of freedom) a function of the coordinates of the system and choosing the CVs is the essence of metadynamics. In ideal CVs, the initial state, the final state, and all the intermediate states of the process are all well defined. As the cost of adding potential to a higher-dimensional space increases and also the analysis of the higher dimensions becomes difficult, it is ideal to consider less number of CVs. The CVs chosen in our study were the number of backbone hydrogen bonds (N_H) assisting in forming the hairpin and the antiparallel β -RMSD (S_β). We make sure the CVs selected were chosen in such a way that they accurately describe the structural features of the hairpin during the folding-unfolding. The N_H , which accounts for the total number of backbone H-bonds is calculated using the

following equation,

$$N_H = \sum_{ij} \frac{1 - \left(\frac{r_{ij}}{r_0}\right)^6}{1 - \left(\frac{r_{ij}}{r_0}\right)^{12}} \quad (3)$$

where r_{ij} is the distance between the i^{th} and j^{th} atoms and r_0 is taken as 2.5 Å (regular H-bond distance).

An anti-parallel β -sheet structure is formed when three adjoining residues from two protein segments are linked by at least three hydrogen bonds and separated by at least two residues to form a turn between them. As well as providing a list of all possible six residue sections that may form an antiparallel beta-sheet, S_β computes the structural deviation between the conformation of the system at any instant and an ideal antiparallel β -sheet structure based on their RMSD. They can be defined as,

$$S_\beta = \sum_i n[RMSD] \quad (4)$$

$$n[RMSD] = \frac{1 - \left(\frac{RMSD}{s_f}\right)^8}{1 - \left(\frac{RMSD}{s_f}\right)^{12}} \quad (5)$$

(ii) Algorithm

Let S be a set of d functions of the microscopic coordinates R of the system

$S(R) = (S_1(R), \dots, S_d(R))$. At any time, the external bias potential added to the system is given by

$$V_G(S(R), t) = \omega \sum_{t=0, \tau, 2\tau} e^{-\frac{(S(R) - S(t'))^2}{2\sigma^2}} \quad (6)$$

where $\omega = W/\tau$

W = Gaussian height

τ = deposition stride

σ = Gaussian width.

As one adds bias potential to the system, the underlying potential starts to grow eventually filling the free-energy basin causing the system to emerge out of the local minima. Finally, when all the free-energy basins are filled by the bias potential, the system resembles a random walk that becomes diffusive in CV space.

(iii) Reconstruction of Free Energy Surface

In the course of time, once the system becomes diffusive, it can be observed that the shape of the potential remains constant, while the value begins to fluctuate around a mean value after a time t_{fill} . A meaningful value can be obtained by averaging the bias potential after t_{fill} based on the equation

$$\bar{V}_G(S(R), t) = \frac{1}{t - t_{fill}} \sum_{t'=t_{fill}}^t V_G(S(R), t') \quad (7)$$

Or in other words the bias potential converges when t tends to infinity and the underlying free energy surface of the system can be calculated as

$$\bar{V}_G(S(R), t \rightarrow \infty) = -\bar{F}(S) + C^{24} \quad (8)$$

or

$$\bar{F}(S) = -\bar{V}_G(S(R), t \rightarrow \infty) + C \quad (9)$$

where C is an irrelevant additive constant

Following the 2 ns NVT equilibration of the three systems (zero external bias, uneven external bias and uniform forces of random orientations), well-tempered MTD simulation of 1 μ s were performed in each case. The trajectory was recorded every 100 steps with a time step of 2 fs. A history-dependent Gaussian potential with 0.1 kJ/mol were deposited on the potential surface along the two CVs every 1000 steps. Gaussian width of 0.1 and 0.5 were chosen for N_H and S_β respectively.

IV. CONVERGENCE OF METADYNAMICS SIMULATION

It is of utmost importance in MTD simulations to look at the convergence of the simulation so as to get a precise assessment of the free energy. Convergence is said to be attained when the free energy does not vary remarkably after a certain period of simulation time. The convergence of free energies along the two CVs (N_H and S_β) for the systems under different force scenarios are shown below. The free energy surface along a single CV is reconstructed from the HILLS file obtained for 1 μ s MTD simulation. Each CV which is not specified for the output is integrated out with the Boltzmann weight $K_B T$ while reconstruction.

A. TrpZip2 β -Hairpin in Solvent

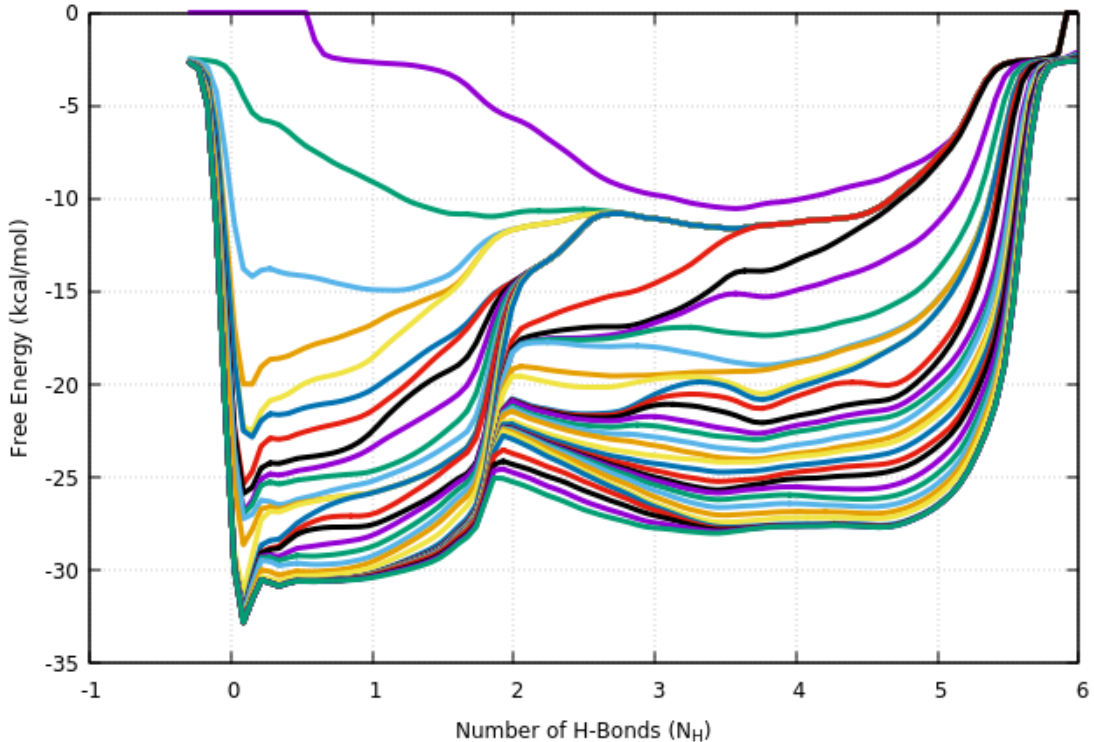


FIG. S4: The convergence of the free energy surface along the backbone H-bonds (N_H) collective variable over the complete metadynamics simulation when the hairpin is in solution and there is no external bias on the protein. A two state folding-unfolding is clearly visible in here.

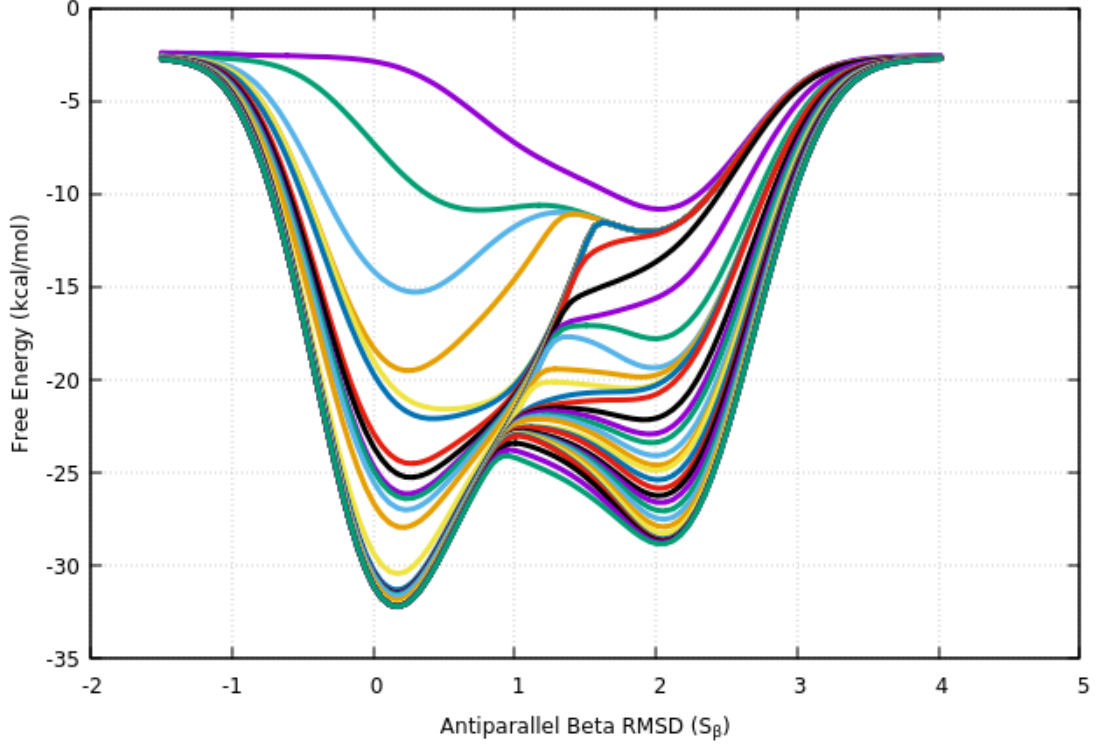


FIG. S5: The convergence of the free energy surface along the antiparallel beta RMSD (S_β) collective variable over the complete metadynamics simulation when the hairpin is in solution and there is no external bias on the protein. Complementary to the (N_H) collective variable under zero external force, this CV also confirms a two state folding-unfolding of the TrpZip2 β -Hairpin.

Fig. S4 and S5 traces the convergence of the free energies along N_H and S_β respectively. Sufficient overlaying of the free energy curves along both the CVs confirms the convergence of the MTD simulations. It is quite evident from the free energy surface (Fig. S4 and S5) that the TrpZip2 β -Hairpin, in the absence of any external bias, folds and unfolds via a two-step mechanism where the protein transits from a folded to an unfolded conformation via a single transition state. N_H value of 5 and S_β value of 2 represents a folded state and N_H value of 0 and S_β value of 0 represents an unfolded state. The transition state is described by $N_H \sim 2$ and $S_\beta \sim 1$.

B. Hairpin in Solvent and Under the Influence of a 30 pN External Tensile Force

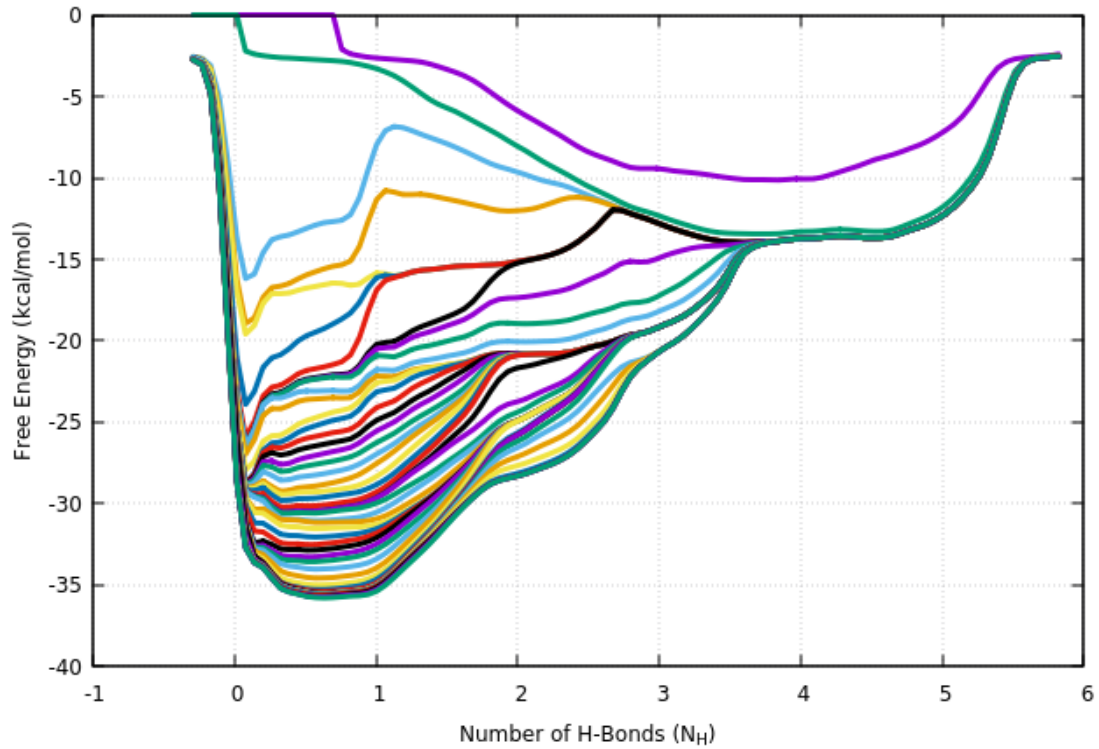


FIG. S6: The convergence of the free energy surface along the backbone H-bonds (N_H) collective variable over the complete metadynamics simulation when the TrpZip2 β -Hairpin experience an external tensile force (\mathbf{F}_0) of 30 pN acting on the C_α atoms of the end residues. Unlike in the case of the system under zero external bias, a stepwise folding-unfolding process is clearly visible in here.

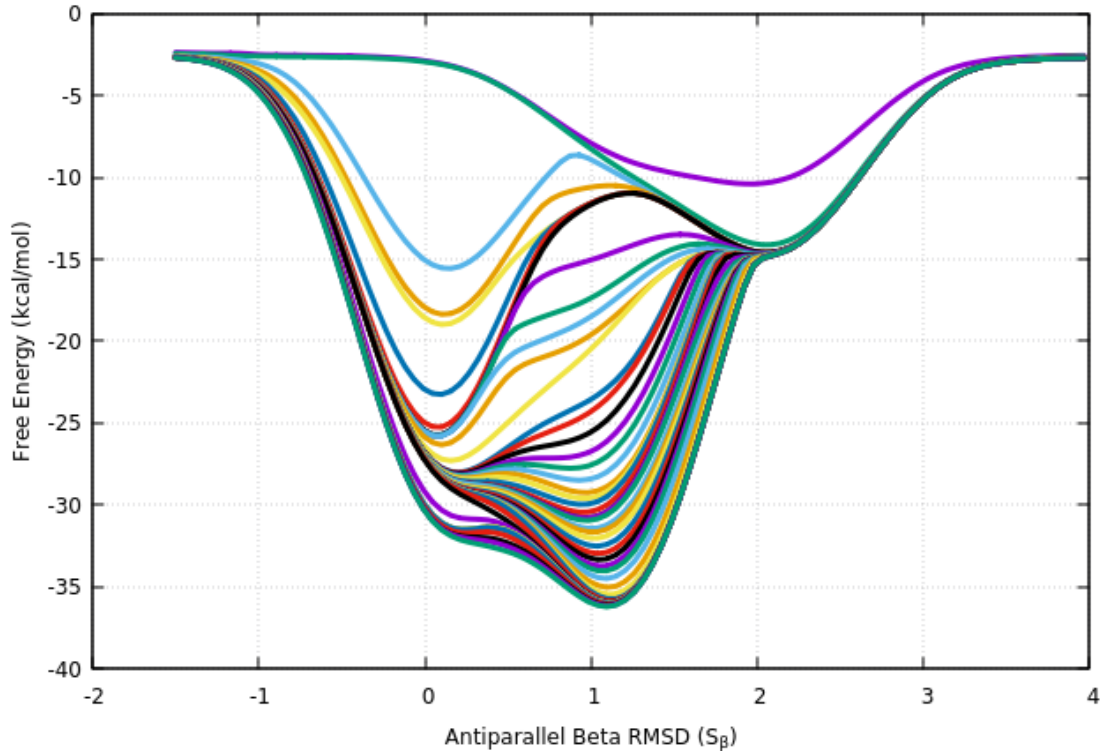


FIG. S7: The convergence of the free energy surface along the antiparallel beta RMSD (S_β) collective variable over the complete metadynamics simulation when the TrpZip2 β -Hairpin experience an external tensile force (\mathbf{F}_0) of 30 pN acting on the C_α atoms of the end residues. This also compliments the inference in Fig. S6.

Fig. S6 and S7 traces the convergence of the free energies along N_H and S_β respectively. Sufficient overlaying of the free energy curves along both the CVs confirms the convergence of the MTD simulations. It is quite evident from the free energy surface (Fig. S6 and S7) that the TrpZip2 β -Hairpin in the presence of an uneven end tensile force of 30 pN folds via a stepwise downhill mechanism with various intermediates. N_H captures the stepwise unfolding while the S_β clearly apprehends the local intermediate being formed.

C. Under the Influence of Uniform Force of Random Orientation

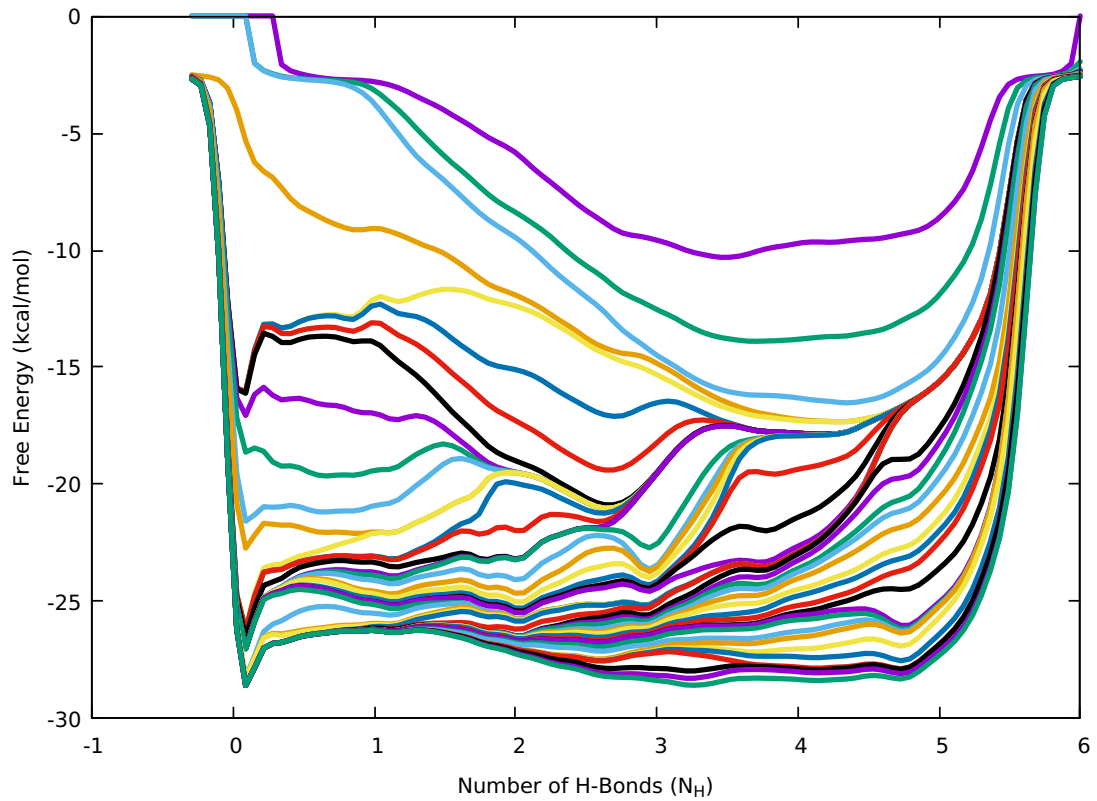


FIG. S8: The convergence of the free energy surface along the backbone H-bonds (N_H) collective variable over the complete metadynamics simulation when the TrpZip2 β -Hairpin experience a uniform random forces of 4 pN over the entire structure .

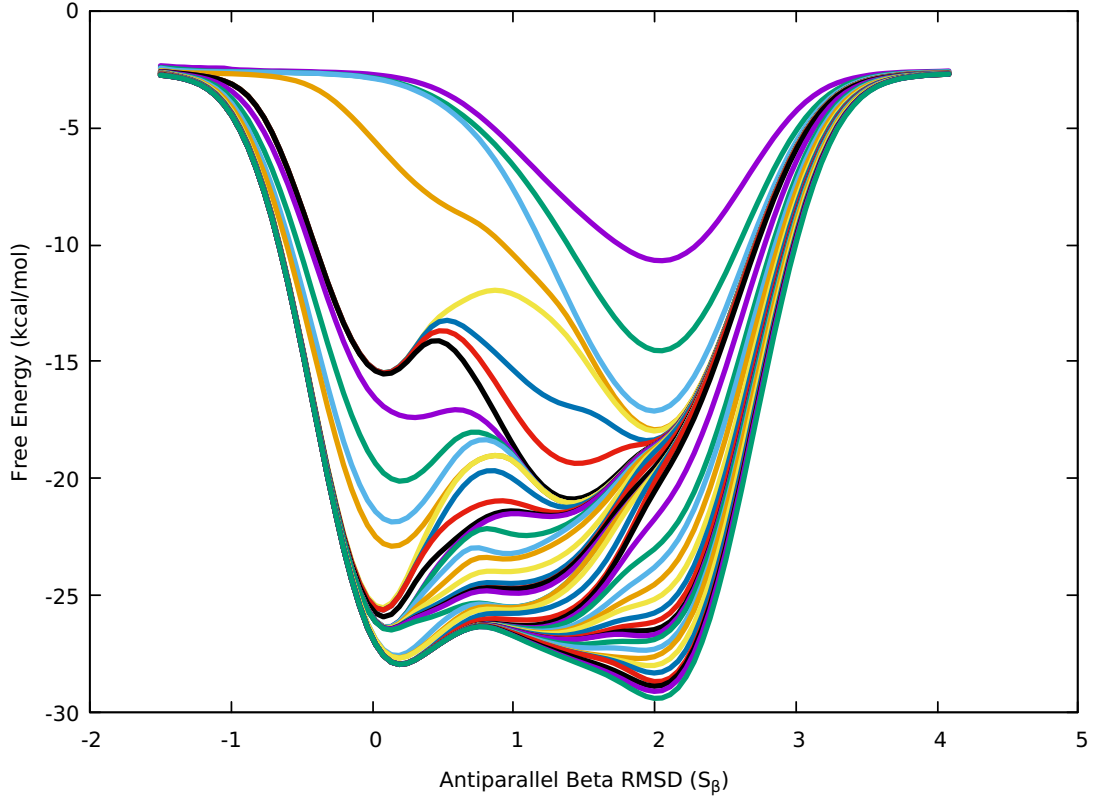


FIG. S9: The convergence of the free energy surface along the antiparallel beta RMSD (S_β) collective variable over the complete metadynamics simulation when the TrpZip2 β -Hairpin experience a uniform random forces of 4 pN over the entire structure.

Fig. S8 and S9 traces the convergence of the free energies along N_H and S_β respectively under uniform force of 4 pN oriented randomly on the hairpin so as to nullify any net force acting on the hairpin and hence recreate a scenario of zero external bias. Sufficient overlaying of the free energy curves along both the CVs confirms the convergence of the MTD simulations. It is quite evident from the free energy surface (Fig. S8 and S9) that the hairpin folds via a two-step mechanism where the protein advances from a folded state to an unfolded one via a single transition state. Thus the convergence of CVs were analyzed for all the systems and it was found that the free energies of the CVs have converged and that each systems have visited all the the folded, unfolded, the transition state and the intermediates sufficiently and hence converged.

V. COMPARISON OF THE FREE ENERGY LANDSCAPE UNDER VARYING EXTERNAL FORCE SCENARIOS

Three dimensional free energy landscape as a function of N_H and S_β obtained for 1 μ s MTD simulation for the different force scenarios is shown in Fig. S10. The unit of free energy is kcal/mol. Fig. S10(a) describes the FES obtained when the protein is under no external bias. This clearly describes a two-step mechanism for the folding-unfolding of TrpZip2 β -Hairpin. The hairpin folds from an unfolded to a folded conformation via a single transition state. Fig. S10(b) describes the FES obtained when the protein experiences an external tensile force of 30 pN which affirms an uneven force acting on the hairpin residue. The protein exhibits an unfolding event with the system getting trapped in distinct intermediate state at lower N_H and S_β values. Fig. S10(c) describes the FES obtained when the protein experiences a uniform forces 4 pN of random orientations over its entire structure so that the net force experienced by the system is overall nullified. Again it is visible that the protein folds via a two-step mechanism just like the zero external bias scenario. This confirms that TrpZip2 β -Hairpin prefers a two-step mechanism for folding-unfolding in solution phase when the net external bias experienced by them is zero.

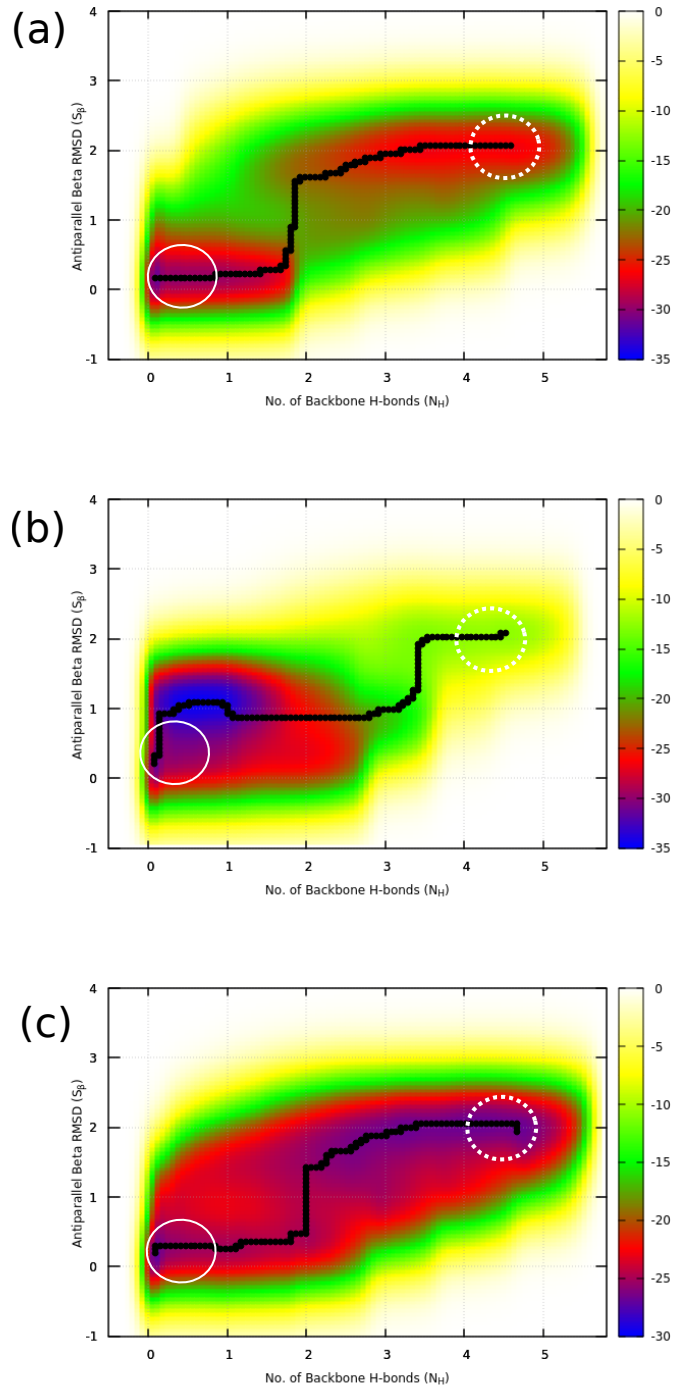


FIG. S10: Comparison of the free-energy landscape obtained from the well-tempered metadynamics simulation for TrpZip2 β -Hairpin as a function of backbone H-bonds (N_H) and antiparallel beta RMSD (S_β) (a) with no external bias in solution (b) 30 pN end tensile force acting on the end residues and (c) Uniform forces with random orientations. Minimum energy path for the folding-unfolding is demonstrated by the black dotted line in all the cases. The dashed and solid circle represent the folded and unfolded states respectively.

VI. TrpZip2 β -HAIRPIN AND ITS FOLDING-UNFOLDING MECHANISM

Hydrophobic group collapse and the formation of the backbone H-bonds are considered to be the key factors determining the formation and detachment of any protein secondary fold. Towards identifying the role played by the hydrophobic groups and backbone hydrogen bonds during the folding–unfolding process of TrpZip2 β -Hairpin, we identified and analyzed, (i) The free energy surface from 1 μ s MTD trajectory along d_1 (distance between TRP2 and TRP11) and d_2 (distance between TRP4 and TRP9) that define the hydrophobic core groups. (ii) All the individual backbone hydrogen bonds with respect to H_1 (see Fig. S1 for description). The behavior of d_1 and d_2 and the evolution of individual backbone hydrogen bonds formation under different scenarios towards the folding–unfolding events were analyzed and summarized below.

A. TrpZip2 β -Hairpin in Solvent

Fig. S11 shows the evolution of d_1 with respect to d_2 while the hairpin undergoes folding–unfolding in SPC/E water. It is observed that the motion of the hydrophobic groups (TRP2–TRP11 and TRP4–TRP9) in TrpZip2 β -Hairpin undergoing a folding–unfolding process along d_1 - d_2 in an externally unbiased situation is diagonal and hence a concerted process. By identifying the motion of the hydrophobic groups while undergoing the hairpin folding–unfolding, we get some insights over the folding–unfolding mechanism. The sequential mechanism for the folding–unfolding process can be nailed via observing the knitting of the backbone H-bonds. Fig. S12 shows the evolution of all the backbone H-bonds with respect to H_1 (H_7 , salt bridge interaction was also considered to assess the correlation of all the backbone H-bonds) while the hairpin undergoes folding–unfolding process. Monitoring H_6 - H_1 and H_5 - H_1 , it can be observed that H_6 and H_5 preferentially collapses with respect to H_1 , thus indicating the selective formation of the hairpin turn while initiating the folding process. Further, we also observed the behavior of H_4 , H_3 , H_2 and H_7 (salt bridge) in comparison to H_1 . Their motions were found to be more or less a concerted process suggesting a zip-out mechanism with hairpin turn forming first and then the concerted knitting of the hairpin leg. Similarly, for the unfolding process, the H-bonds H_1 to H_4 including H_7 opens up in a concerted fashion. All these suggests a two-step mechanism which involves the for-

mation of the turn to concerted closing up of all the backbone H-bonds along the hairpin legs.

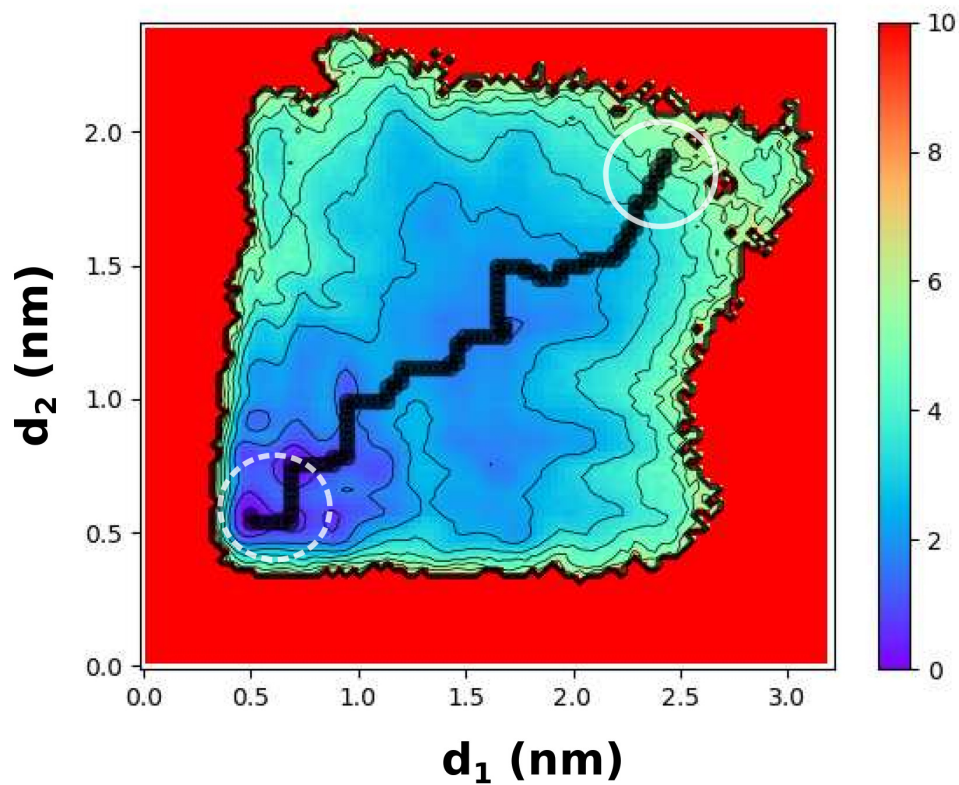


FIG. S11: The evolution of d_2 with respect to d_1 (see Fig. S1 for details) as captured from the metadynamics trajectory during the folding-unfolding process of TrpZip2 β -hairpin while in the solution phase. A diagonal mean free energy path (black line) justifies a concerted motion of the hydrophobic groups during the folding-unfolding process while in the solution. The dashed and solid circle represent the folded and unfolded states respectively.

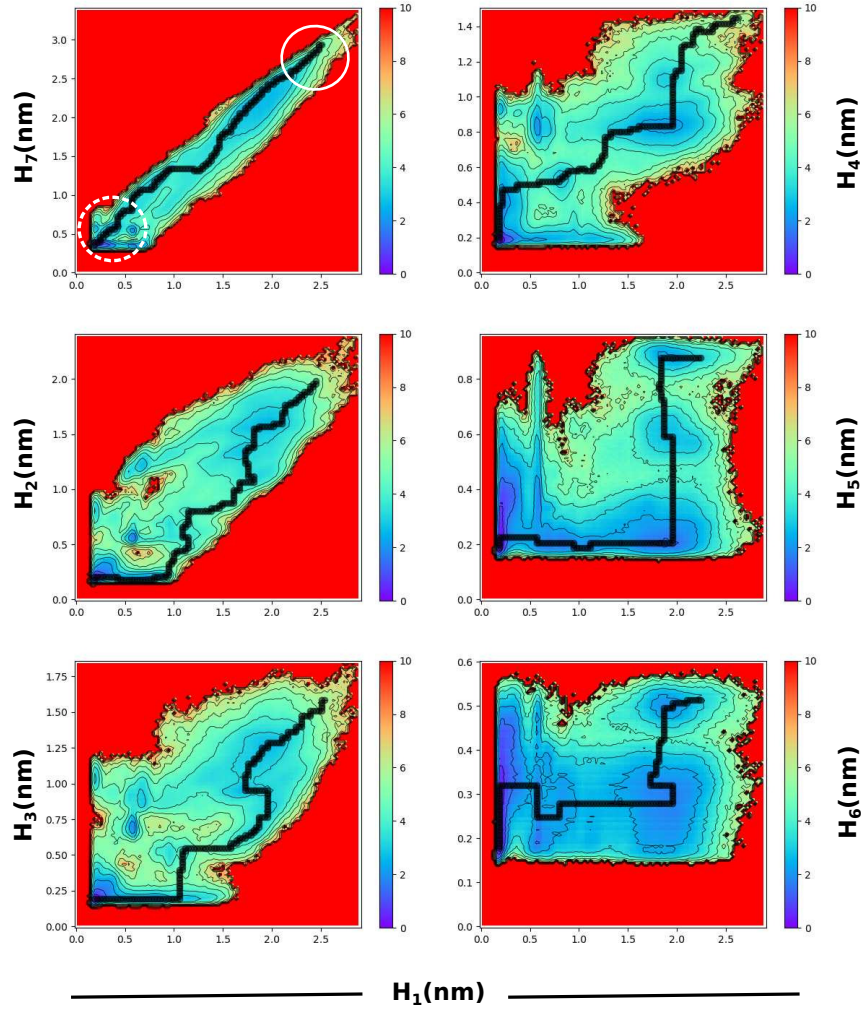


FIG. S12: The free energy landscape obtained from metadynamics trajectory for TrpZip2 β -Hairpin which demonstrates the evolution of the individual backbone H-bonds (H_n , different n 's can be identified in Fig. S1) with respect to H_1 with no external bias acting on the end residues of the hairpin. Minimal path for H-bond evolution along H_1 - H_n is demonstrated by the black dotted line. The dashed and solid circle represent the folded and unfolded states respectively. The definition upholds for folded and unfolded states in all the subplots.

B. Hairpin in Solvent and Under the Influence of a 30 pN External Tensile Force

Fig. S13 shows the evolution of d_1 with respect to d_2 while the hairpin undergoes folding-unfolding in SPC/E water with an external tensile force of 30 pN so as to mimic the unbalanced forces acting on the TrpZip2 β -Hairpin. In contrast to the unbiased case, it is observed here that the motion of the hydrophobic groups or the hydrophobic collapse (TRP2–TRP11

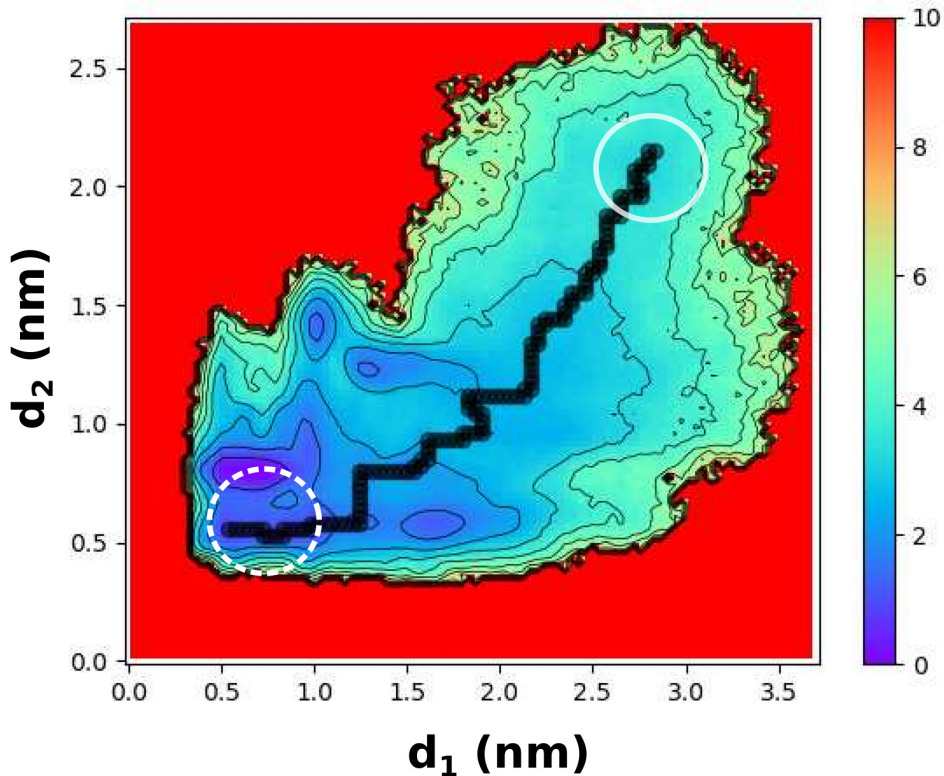


FIG. S13: The evolution of d_2 with respect to d_1 (see Fig. S1 for details) as captured from the metadynamics trajectory during the folding-unfolding process of TrpZip2 β -Hairpin while in the solution phase and a 30 pN tensile force acting on the end residues. Unlike the zero external force situation, the mean free energy path (black line) propagates along d_1 first and then opens the d_2 . Justifiably, the small end force do interferences with the movement of the hydrophobic groups during the folding-unfolding process of the TrpZip2 hairpin. The dashed and solid circle represent the folded and unfolded states respectively.

and TRP4–TRP9) in TrpZip2 β -Hairpin undergoing a folding-unfolding process along d_1 - d_2 is not diagonal. d_1 - d_2 plot develops along d_1 first, opening the hairpin leg initially and

further along d_2 taking the hairpin to a random coil. Thus a sub-pico-newton level tensile force readily influences the motion of the hydrophobic core groups making it a non-concerted process, mostly populating different intermediate states and thereby deviating from the proposed two-step mechanism.

Having seen that the d_1 - d_2 motion is significantly different from the externally unbi-

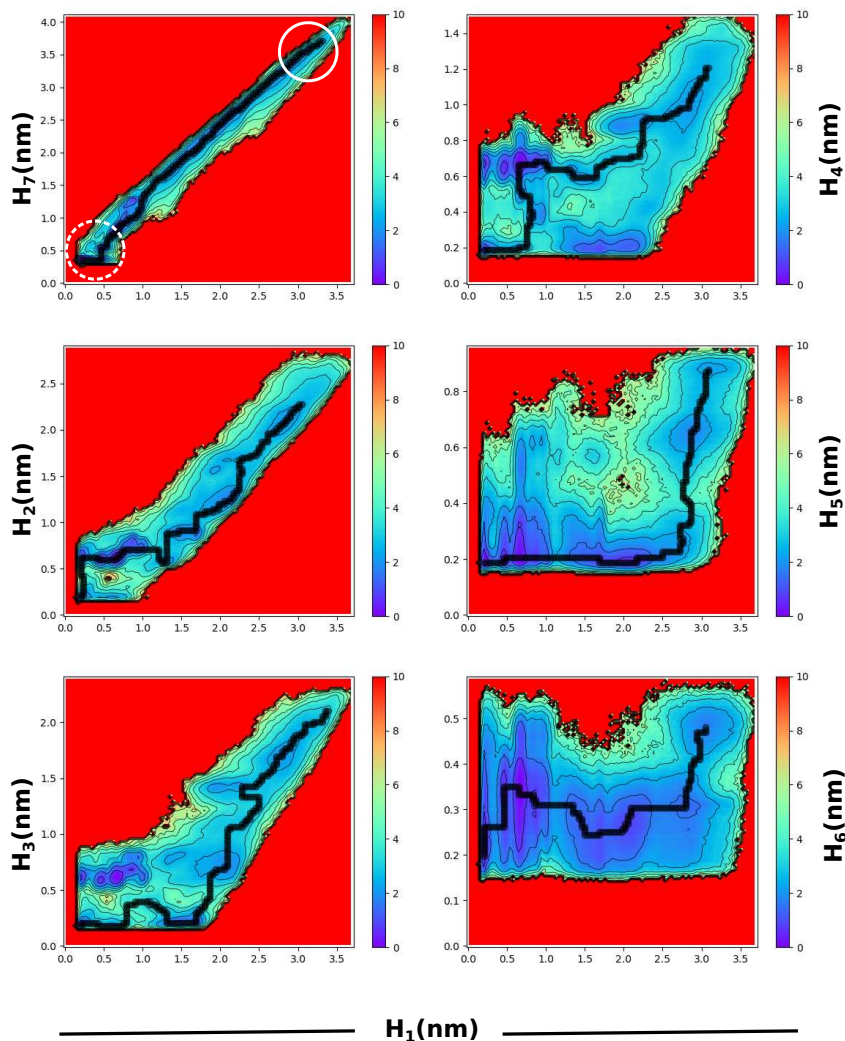


FIG. S14: The free energy landscape obtained from metadynamics trajectory for TrpZip2 β -Hairpin which demonstrates the evolution of the individual backbone H-bonds (H_n , different n 's can be identified in Fig. S1) with respect to H_1 with 30 pN tensile force acting on the end residues. Minimal path for H-bond evolution along H_1 - H_n is demonstrated by the black dotted line. The dashed and solid circle represent the folded and unfolded states respectively. The definition upholds for folded and unfolded states in all the subplots.

ased hairpin, it is yet again worth assessing the backbone H-bonds to decipher the folding-unfolding mechanism. Fig. S14 establishes the evolution of all the H-bonds with respect to H_1 while the hairpin undergoes folding-unfolding in presence of a tensile force of 30 pN. On monitoring the H_5 - H_6 and H_6 - H_1 evolution, it can be observed that H_6 and H_5 preferentially collapses with respect to H_1 , thus indicating the selective formation of the hairpin turn while initiating the folding process. Further, we also assessed the behavior of H_4 , H_3 , H_2 and H_7 in comparison to H_1 . H_7 (salt bridge) is found to be concerted with respect to H_1 suggesting that they make and break together. Unlike the unbiased system, the behavior of H_4 , H_5 , and H_6 are found to be a stepwise process, which justifies the formation of different intermediate states here. Further, H_1 , H_2 and H_3 open in a concerted fashion. Hence two-step mechanism is ruled out here, with the folding-unfolding dominated by multiple intermediate states.

C. Hairpin in Solvent and Under Uniform Forces of Random Orientation

Thus having seen the distinct behavior of the TrpZip2 β -Hairpin under both externally unbiased and also in the presence of an external tensile force, it would be great if one of the situations can be validated by a different method so as to affirm our findings. Thus to realize the unbiased hairpin state, hairpin was exposed to uniform force of 4 pN randomly oriented along the hairpin backbone. This mimics an unbiased state of hairpin in solvent. Fig. S15 shows the evolution of d_1 with respect to d_2 for folding-unfolding of

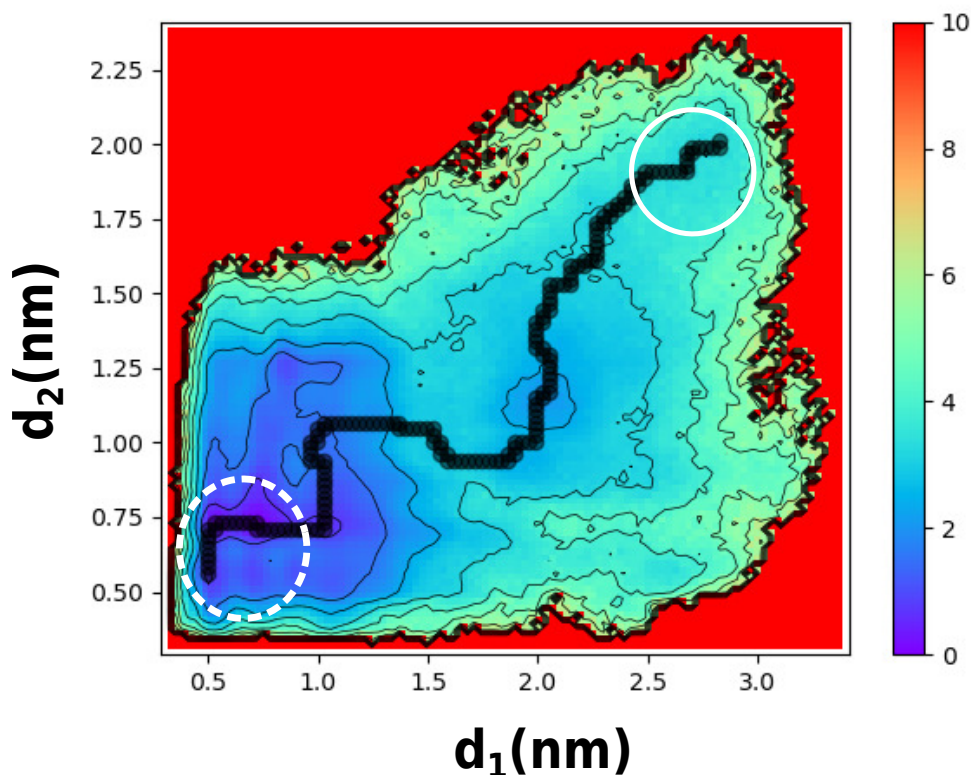


FIG. S15: The evolution of d_2 with respect to d_1 (see Fig. S1 for details) as captured from the metadynamics trajectory during the folding-unfolding process of TrpZip2 β -Hairpin while in the solution phase and a 4 pN random force acting over the entire structure. Minimal path for H-bond evolution along H_1-H_n is demonstrated by the black dotted line. The dashed and solid circle represent the folded and unfolded states respectively.

hairpin in water, while it is exposed to uniform forces of 4 pN of random orientations. It can be visualized that the motion of the hydrophobic group or the hydrophobic collapse

(TRP2–TRP11 and TRP4–TRP9) in TrpZip2 β -Hairpin undergoing a folding-unfolding process along d_1 - d_2 is mostly diagonal and hence a concerted process. This is similar to the unbiased scenario.

Further, Fig. S16 exhibits the evolution of all the backbone H-bonds with respect to H_1

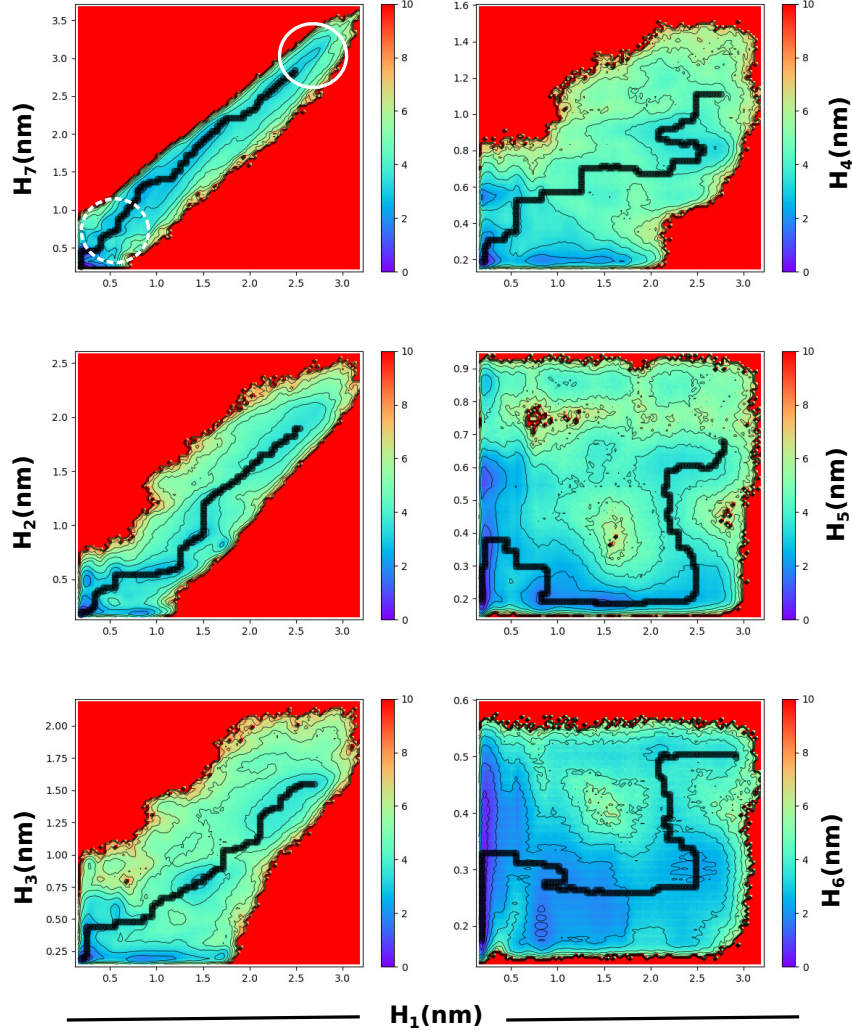


FIG. S16: The free energy landscape obtained from metadynamics trajectory for TrpZip2 β -Hairpin which demonstrates the evolution of the individual backbone H-bonds (H_n , different n 's can be identified in Fig. S1) with respect to H_1 when a uniform random force of 4 pN is acted on the entire hairpin. Minimal path for H-bond evolution along H_1 - H_n is demonstrated by the black dotted line. The dashed and solid circle represent the folded and unfolded states respectively. The definition upholds for folded and unfolded states in all the subplots.

while the hairpin undergoes folding-unfolding process. Again, monitoring H_6 - H_1 and H_5 - H_1 ,

it can be observed that H_5 and H_6 preferentially collapses first with respect to H_1 , thus indicating the selective formation of the hairpin turn while initiating the folding process. The behavior of H_4 , H_3 , H_2 and H_7 in comparison to H_1 , is yet again found to be more or less a concerted process suggesting a zip-out mechanism with hairpin turn forming first and then the concerted knitting of the hairpin leg, which is in line with the externally unbiased hairpin in solvent. Similarly, for the unfolding process, the H_1 to H_4 including H_7 opens up in a concerted fashion and then disrupting the turn. This confirms the two-step mechanism which involves the formation of the turn to concerted closing up of the hairpin legs.

Thus to summarize, it was very well identified and established by more than one method that the overall unbiased hairpin in water exhibits a two-step mechanism for folding-unfolding. The folding process is initiated via the hydrophobic collapse assisted hairpin turn formation and further pinning up the backbone H-bonds in forming the hairpin. The impact of uneven forces on the hairpin initiates the hairpin folding in the same manner by forming the hairpin turn as in the unbiased case, but the pinning up of the backbone H-bonds is a stepwise process populating the misfolded intermediates. Similarly, the unfolding process for the unbiased hairpin is a concerted process while the hairpin under external bias exhibits a stepwise unfolding.

-
- * Electronic address: padmesh@iitpkd.ac.in
- ¹ A. G. Cochran, N. J. Skelton, and M. A. Starovasnik, Proceedings of the National Academy of Sciences **98**, 5578 (2001).
 - ² W. Y. Yang and M. Gruebele, Journal of the American Chemical Society **126**, 7758 (2004).
 - ³ W. Y. Yang, J. W. Pitera, W. C. Swope, and M. Gruebele, Journal of molecular biology **336**, 241 (2004).
 - ⁴ S. R. Durell, B. R. Brooks, and A. Ben-Naim, The Journal of Physical Chemistry **98**, 2198 (1994).
 - ⁵ A. Ben-Naim, Journal of Physical Chemistry **94**, 6893 (1990).
 - ⁶ S. R. Durell and A. Ben-Naim, Biopolymers **107**, e23020 (2017).
 - ⁷ A. G. Cochran, N. J. Skelton, and M. A. Starovasnik, Proceedings of the National Academy of Sciences **98**, 5578 (2001).
 - ⁸ H. J. C. Berendsen, J. R. Grigera, and T. P. Straatsma, Journal of Physical Chemistry **91**, 6289 (1987).
 - ⁹ H. J. C. Berendsen, D. van der Spoel, and R. van Drunen, Computer physics communications **91**, 43 (1995).
 - ¹⁰ B. Hess, C. Kutzner, D. van der Spoel, and E. Lindahl, Journal of chemical theory and computation **4**, 435 (2008).
 - ¹¹ W. L. Jorgensen and J. Tirado-Rives, Journal of the American Chemical Society **110**, 1657 (1988).
 - ¹² W. L. Jorgensen, D. S. Maxwell, and J. Tirado-Rives, Journal of the American Chemical Society **118**, 11225 (1996).
 - ¹³ P. G. Bolhuis, Biophysical journal **88**, 50 (2005).
 - ¹⁴ R. B. Best and J. Mittal, Proteins: Structure, Function and Genetics **79**, 1318 (2010).
 - ¹⁵ S. Nosé, Molecular physics **52**, 255 (1984).
 - ¹⁶ W. G. Hoover, Physical review A **31**, 1695 (1985).
 - ¹⁷ B. Hess, H. Bekker, H. J. C. Berendsen, and J. G. E. M. Fraaije, Journal of the American Chemical Society **18**, 1463 (1998).
 - ¹⁸ T. Darden, D. York, and L. Pedersen, The Journal of chemical physics **98**, 10089 (1993).

- ¹⁹ S. Park and K. Schulten, *The Journal of chemical physics* **120**, 5946 (2004).
- ²⁰ S. Izrailev, S. Stepaniants, B. Isralewitz, D. Kosztin, H. Lu, F. Molnar, W. Wriggers, and K. Schulten, in *Computational molecular dynamics: challenges, methods, ideas* (Springer, 1999), pp. 39–65.
- ²¹ A. Barducci, M. Bonomi, and M. Parrinello, *Wiley Interdisciplinary Reviews: Computational Molecular Science* **1**, 826 (2011).
- ²² R. Martoňák, A. R. Oganov, and C. Glass, *Phase Transitions* **80**, 277 (2007).
- ²³ D. S. Perumalla, G. Govind, and P. Anjukandi, *ChemistrySelect* **5**, 5748 (2020).
- ²⁴ G. Bussi, A. Laio, and M. Parrinello, *Physical review letters* **96**, 090601 (2006).